Newsletters on Stratigraphy, Vol. 44/2, 113–122 **Article**
published online April 2011

Stratigraphic relationships between the last occurrence of *Neogloboquadrina inglei* and marine isotope stages in the northwest Pacific, D/V *Chikyu* Expedition 902, Hole C9001C

Hanako Domitsu[1], Jun-ichi Uchida[2], Kaoru Ogane[3], Nana Dobuchi[4], Tokiyuki Sato[4], Minoru Ikehara[5], Hiroshi Nishi[6], Shiro Hasegawa[7], and Motoyoshi Oda[8]

With 3 figures and 1 table

Abstract. The stratigraphic relationships between the last occurrence (LO) of the planktic foraminiferan *Neogloboquadrina inglei* in the middle Pleistocene and established marine isotope stages (MIS) was investigated using a 365-m-long sediment core from a continental slope in the northwest Pacific near the Shimokita Peninsula, Japan. Two tephra layers (Shikotsu-Daiichi and Aso-4 tephras) and two nannofossil datum planes (first occurrence of *Emiliania huxleyi* and LO of *Pseudoemiliania lacunosa*) were used as age-control points, and the oxygen isotope stratigraphy of Hole C9001C was established by correlating the oxygen isotope values of the benthic foraminiferan *Uvigerina akitaensis* with the standard oxygen isotope curve LR04. Hole C9001C provides the first continuous, high-sedimentation-rate (20–90 cm/kyr) record from MIS 18 to present in the northwestern Pacific near Japan. The stratigraphic position of the LO of *N. inglei* is in late MIS 16 or near the MIS 16/15 boundary.

Key words. planktic foraminifera, biostratigraphy, oxygen isotope stratigraphy, Pleistocene, northwest Pacific.

Author's addresses:
[1] (corresponding author), Department of Ecosystem Studies, School of Environmental Science, The University of Shiga Prefecture, 2500 Hassaka-cho, Hikone 522-8533, Japan. E-Mail: domitsu.h@ses.usp.ac.jp
[2] OYO Corporation, 2-2-19 Daitakubo, Minami-ku, Saitama 336-0015, Japan. Present address: Earthquake and Tsunami Evaluation Group, Seismic Safety Division, Japan Nuclear Energy Safety Oraganization, Kamiya-cho MT Bldg., 4-3-20 Toranomon, Minato-ku, Tokyo 105-0001, Japan. E-Mail: uchida.junichi@jnes.co.jp
[3] Institute of Geology and Paleontology, Graduate School of Science, Tohoku University, 6-3 Aoba, Aramaki, Aoba-ku, Sendai 980-8578, Japan. Present address: Department of Botany, National Museum of Nature and Science, 4-1-1 Amakubo, Tsukuba 305-0005, Japan. E-Mail: ogane@mtc.biglobe.ne.jp
[4] Institute of Applied Earth Sciences, Faculty of Engineering and Resource Science, Akita University, 1-1 Tegatagakuen-machi, Akita 010-8502, Japan. E-Mail: toki@gipc.akita-u.ac.jp
[5] Center for Advanced Marine Core Research, Kochi University, B200, Monobe, Nankoku 783-8502, Japan. E-Mail: ikehara@kochi-u.ac.jp
[6] Department of Natural History Sciences, Graduate School of Science, Hokkaido University, Kita 10, Nishi 8, Kita-ku, Sapporo 060-0810, Japan. Present address: The Center for Academic Resources and Archives, Tohoku University Museum, Tohoku University, 6-3 Aoba, Aramaki, Aoba-ku, Sendai 980-8578, Japan. E-Mail: hnishi@m.tohoku.ac.jp
[7] Department of Earth and Environments, Graduate School of Science and Technology, Kumamoto University, 2-39-1 Kurokami, Kumamoto 860-8555, Japan. E-Mail: shiro@sci.kumamoto-u.ac.jp
[8] Institute of Geology and Paleontology, Graduate School of Science, Tohoku University, 6-3 Aoba, Aramaki, Aoba-ku, Sendai 980-8578, Japan. E-Mail: odam@mail.tains.tohoku.ac.jp

www.borntraeger-cramer.de
DOI: 10.1127/0078-0421/2011/0007
0078-0421/2011/0007 $ 2.50

1. Introduction

The *Neogloboquadrina* group is a common component of mid- to high-latitude planktic foraminiferal assemblages of the late Neogene and is important in establishing the Pliocene and Pleistocene biostratigraphy of these areas. Kucera and Kennett (2000) reported the biochronology of eight neogloboquadrinid events (first and last occurrences) in six Pliocene to Pleistocene deep-sea successions obtained during Ocean Drilling Program (ODP) Leg 167 in the northeast Pacific near California (Fig. 1a). The last occurrence (LO) of *Neogloboquadrina inglei* is the youngest of the Pleistocene biochronological markers, with a mean estimated age of ca. 0.7 Ma (Kucera and Kennett 2000). The LO of *N. inglei* is situated just above the base of the Brunhes normal polarity epoch of ODP Site 1150 in the northwest Pacific (Fig. 1b), and its age is estimated at ca. 0.7 Ma (Domitsu and Oda 2008). In these previous studies, the ages for this bioevent were derived by linear interpolation between the age of the Brunhes/Matuyama boundary (0.78 Ma) and nannofossil datum planes or tephra horizons (Kucera and Kennett 2000; Domitsu and Oda 2008). Detailed correlation of the LO of *N. inglei* with oxygen isotope stages will refine the stratigraphic position and age of this important biohorizon.

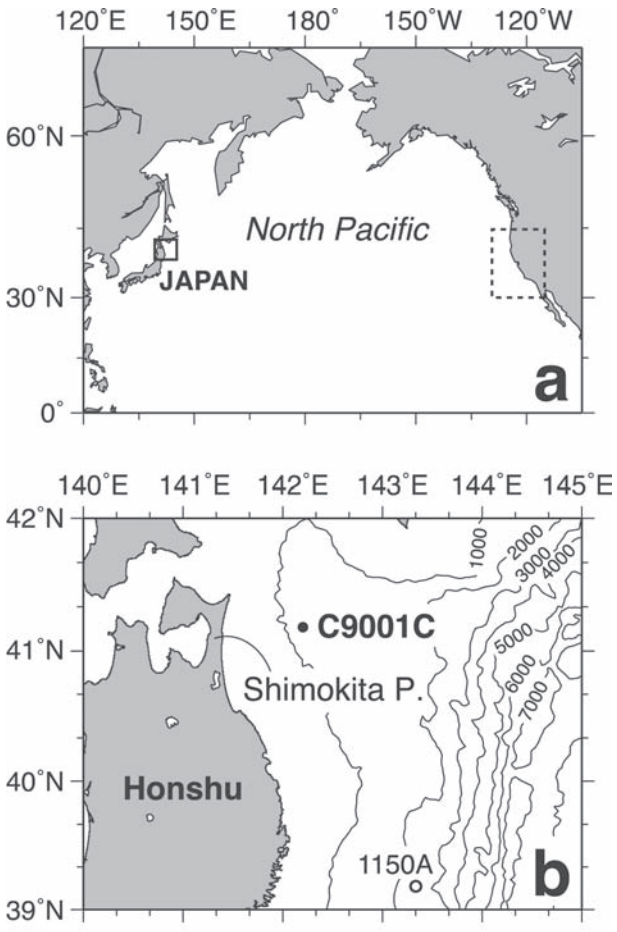

Fig. 1. (a) Locations of the study areas: solid rectangle, this study; dotted rectangle, Kucera and Kennett (2000). (b) Seafloor topography in the study area showing core locations: solid circle, Hole C9001C used in this study; open circle, ODP Hole 1150A examined by Domitsu and Oda (2008).

In 2006, the CK06-06 D/V *Chikyu* Shakedown Cruise was undertaken near the Shimokita Peninsula, Japan. Site C9001 Hole C was drilled on the continental slope at 1180 m water depth (41° 10′ 38.28″ N, 142° 12′ 04.86″ E; Fig. 1b). Shipboard and shore-based preliminary study of siliceous and calcareous microfossil biostratigraphy, tephrostratigraphy, and magnetostratigraphy suggest that the 365-m-long core from Hole C9001C records a high and continuous sedimentation rate during the Brunhes normal polarity epoch (Aoike 2008; Kobayashi et al. 2009). Hole C9001C material has a strong potential to reveal detailed relationships among biostratigraphic events and oxygen isotope stages in the middle to late Pleistocene. This study establishes the planktic foraminiferal and calcareous nannofossil biostratigraphy and oxygen isotope stratigraphy of Hole C9001C and improves the stratigraphic position of the LO of *N. inglei*.

2. Materials and methods

Hole C9001C sediment consists predominantly of olive-black to dark olive-gray, diatomaceous silty clay containing microfossils such as siliceous sponge spicules, foraminifera, radiolaria, calcareous nannofossils, and silicoflagellata (Kobayashi et al. 2009; Fig. 2). Tephra and sand layers are common at 0–158 m below the seafloor (mbsf) and 348–365 mbsf and are generally several centimeters thick. The tephra layer at 30.30–30.39 mbsf was correlated with the Shikotsu-Daiichi tephra (Spfa-1), and the tephra layer at 54.35–54.38 mbsf was correlated with the Aso-4 tephra (Aoike et al. 2010; Fig. 2). Thick layers of loose, fine- to medium-grained lithic sand are present between 340 and 348 mbsf. Slumps and debrites are present at 124–135 mbsf and 203–207 mbsf (Aoike 2008). Paleomagnetic measurements indicate that the entire interval intersected by Hole C9001C is in the

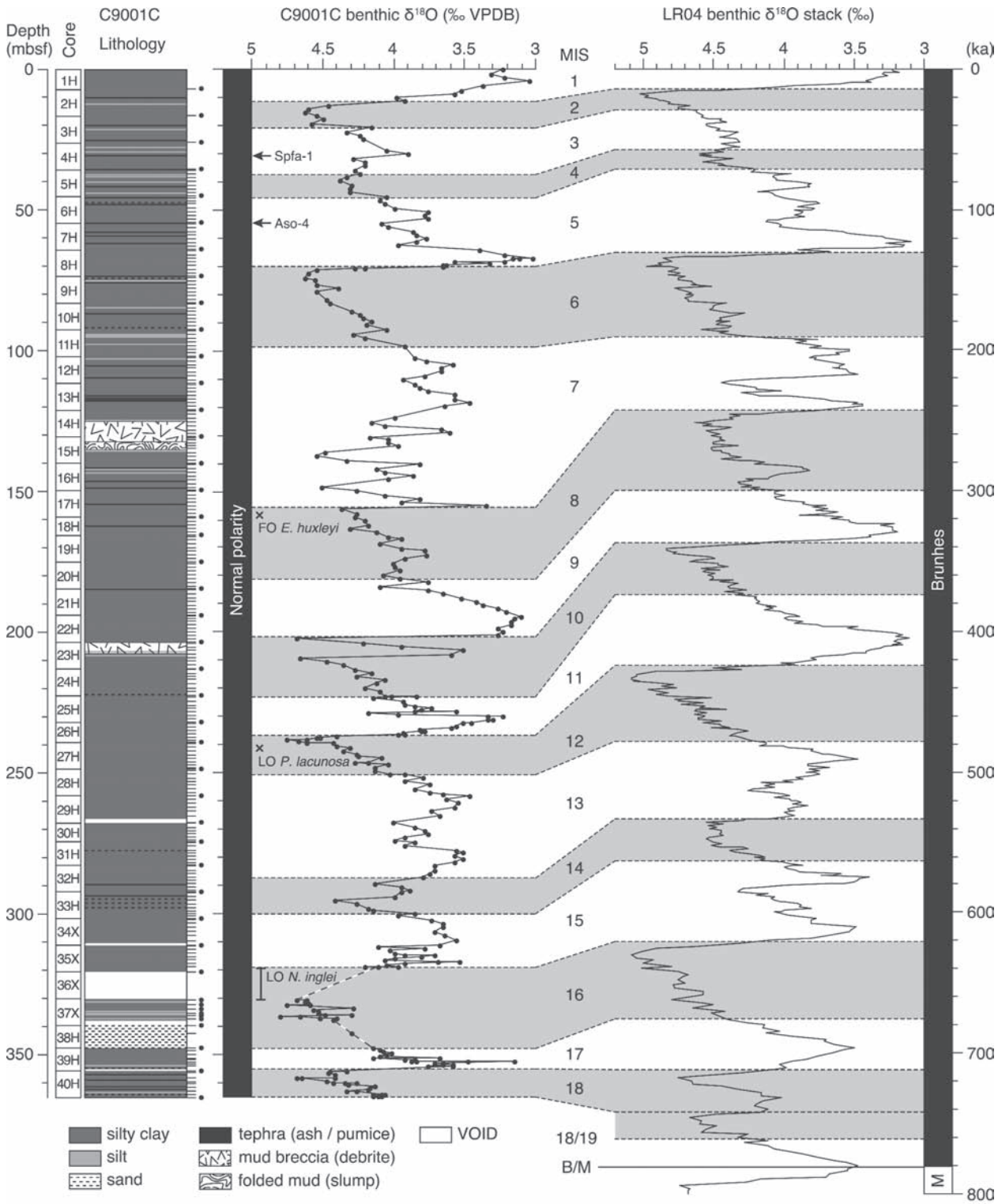

Fig. 2. Oxygen isotope stratigraphy of core C9001C based on correlation of the oxygen isotope record of benthic foraminifera with the standard $\delta^{18}O$ curve of Lisiecki and Raymo (2005). Glacial stages are shaded. "B/M" indicates the Brunhes/Matuyama boundary. Markers on the right side of the lithologic columnar section denote horizons sampled for microfossil analyses: solid circles, planktic foraminifera; bars, calcareous nannofossils.

Brunhes epoch of normal polarity, implying that sediment at the base of the cored interval is younger than 780 ka (Kobayashi et al. 2009).

Core sediment was collected at 0.5–1.5-m intervals (1–4 samples/section), yielding a total of 385 samples. Each sample was freeze-dried and washed through a 63-μm screen. Residues were dried at ca. 40°C and then divided into aliquots containing at least 300 foraminiferal specimens using a microsplitter. The benthic foraminiferan *Uvigerina akitaensis* is abundant and well to moderately preserved in this core. Approximately three specimens (500–800 μm diameter) were selected from each of the 385 samples for stable isotope analysis. *Uvigerina akitaensis* is not present at 202.35 mbsf, and so *Uvigerina peregrina*, a related species, was used for that interval. Benthic foraminiferal tests were cracked and cleaned in an ultrasonic cleaner with methanol to remove mud adhering to their chamber walls. Measurements were made using an online system employing an IsoPrime isotope-ratio mass spectrometer (GV Instruments Ltd.) coupled to a Multicarb automatic sample treatment system at the Center for Advanced Marine Core Research, Kochi University, Japan. Isotopic values are expressed as per mil (‰) relative to the Vienna Pee Dee Belemnite (VPDB) standard. The analytical precision is ± 0.07‰ for $\delta^{18}O$.

For planktic foraminiferal biostratigraphy, planktic foraminifera larger than 125 μm were picked from the divided residues and identified under a Zeiss Stemi 2000-C stereomicroscope. For calcareous nannofossil analysis, smear-slides were studied using a Zeiss Axio Imager polarizing microscope at 1600x magnification.

3. Results and discussion

Oxygen isotope values for benthic foraminifera from 340 horizons in Hole C9001C showed cyclic changes through the length of the core, ranging from 3.0 to 4.8‰ (Fig. 2; Appendix 1).

The chronological framework of core C9001C was established using tephrostratigraphy and nannofossil biostratigraphy. The Spfa-1 and Aso-4 tephras have been used as critical time-markers in and around Japan (Machida 1999). The Spfa-1 tephra is correlated with marine isotope stage (MIS) 3 (Aoki and Arai 2000), and the Aso-4 tephra with MIS 5b (Aoki 2007). The first occurrence (FO) of *Emiliania huxleyi* is between 157.72 and 158.91 mbsf (Fig. 2). *Pseudoemiliania lacunosa* occurred consistently below 242.14 mbsf; the LO of this species is between 240.71 and 242.14 mbsf (Fig. 2). Wei (1993) and Sato et al. (1999) reported the FO of *E. huxleyi* in MIS 8, and the LO of *P. lacunosa* in MIS 12. Raffi et al. (2006) summarized the detailed positions of these biohorizons relative to the oxygen isotope stratigraphy using magnetic reversal and stage boundary ages based on ATNTS2004 (Lourens et al. 2004). Sato et al. (2009) studied a high-resolution Quaternary succession from Integrated Ocean Drilling Program (IODP) Site U1308 in the North Atlantic Ocean and found the stratigraphic positions of both the FO of *E. huxleyi* and the LO of *P. lacunosa* just below the highest peaks in $\delta^{18}O$ values during MIS 8 and 12, respectively. Using these two nannofossil datum planes and two tephra layers as age-control points, the oxygen isotope curve of C9001C can be correlated with the standard oxygen isotope curve LR04 (Lisiecki and Raymo 2005). Stratigraphic variation in the oxygen isotope record of C9001C is in good agreement with the standard LR04 curve, with some minor differences. Drastic decreases and increases in isotopic values mark stage boundaries, as proposed by Shackleton and Opdyke (1973). Eighteen marine isotope stages (MIS 18 – 1) are recognized in C9001C (Fig. 2). An excursion of 1 ‰ in $\delta^{18}O$ data during late MIS 10 is probably associated with a debrite between 203 and 207 mbsf. The $\delta^{18}O$ values in early to middle MIS 7 are not well correlated with the LR04 values for this interval, probably because of slumps and debrites between 124 and 135 mbsf.

The depth-age relationship of C9001C is well constrained by the calculated ages of MIS boundaries using LR04 (Fig. 3a; Table 1). The sedimentation rate excluding reworked layers ranged from 20 to 90 cm/kyr, with an average of ca. 50 cm/kyr (Fig. 3b). Hole C9001C is the first example of a succession from near Japan in the northwestern Pacific that has an apparently high sedimentation rate and that provides a nearly continuous record from MIS 18 to present during the Brunhes normal polarity epoch.

The LO of *N. inglei* in the middle Pleistocene is located between 320.66 and 330.59 mbsf in core C9001C. Based on the chronology of C9001C, this event appears to have taken place in late MIS 16 or near the MIS 16/15 boundary (Fig. 2). The $\delta^{18}O$ values between 330 and 340 mbsf are nearly as high as the highest peaks at the glacial maximum of MIS 12. The age of this bioevent is bracketed by the MIS 17/16 and 16/15 boundaries (Table 1). Based on linear interpolation (excluding thick sand layers at 340–348 mbsf), the age of the LO of *N. inglei* is estimated

to be between 626 and 652 ka. This is slightly younger than previous estimates of 0.712 ± 0.021 Ma from six sites near California (Kucera and Kennett 2000) and 0.73 ± 0.05 Ma in the northwest Pacific (Domitsu and Oda 2008). This age difference may be explained by the previous studies having fewer magnetostratigraphic, tephrostratigraphic, and biostratigraphic controls available for the interval between 0.8 Ma and the present. Kucera and Kennett (2000) assigned ages to this event using linear interpolation between the nearest lower and higher age-control points, which were the base of the Brunhes normal polarity epoch (0.78 Ma) and the LO of *P. lacunosa* (0.46 Ma; Fornaciari 2000). Domitsu and Oda (2008) used the ages of the base of the Brunhes (0.78 Ma) and the Aso-4 tephra (0.09 Ma; Oba 1991; Machida 1999) as age-control points, assuming constant sedimentation rates.

Kucera and Kennett (2000) provided ages for this event from multiple sites off the coast of California (Fig. 1a). Almost all of these dates cluster around 0.7–0.75 Ma, although one is younger than 0.6 Ma. They pointed out that Site 1011 with the younger age has the weakest age model, which is clearly the reason for the unusual age estimate. Observations in the present study also suggest that this young age at Site 1011 is inaccurate, and support a narrow, basin-wide synchronicity for this event along the California margin.

Neogloboquadrina inglei is a new species formally described in Kucera and Kennett (2000), and little knowledge exists of the stratigraphic and spatial distributions of this species in the Pacific. Detailed correlation of the LO of *N. inglei* with oxygen isotope stages at additional sites will show the timing of the Pacific-wide occurrence of this species.

Table 1 The 18 age-control points used in this study.

Depth (mbsf)	MIS boundary	Age (ka) LR04
11.21	1/2	14
20.91	2/3	29
37.10	3/4	57
45.69	4/5	71
69.97	5/6	130
98.15	6/7	191
155.73	7/8	243
180.93	8/9	300
201.71	9/10	337
222.48	10/11	374
236.53	11/12	424
250.63	12/13	478
287.03	13/14	533
299.87	14/15	563
318.62	15/16	621
347.74	16/17	676
355.13	17/18	712
364.93	–	742

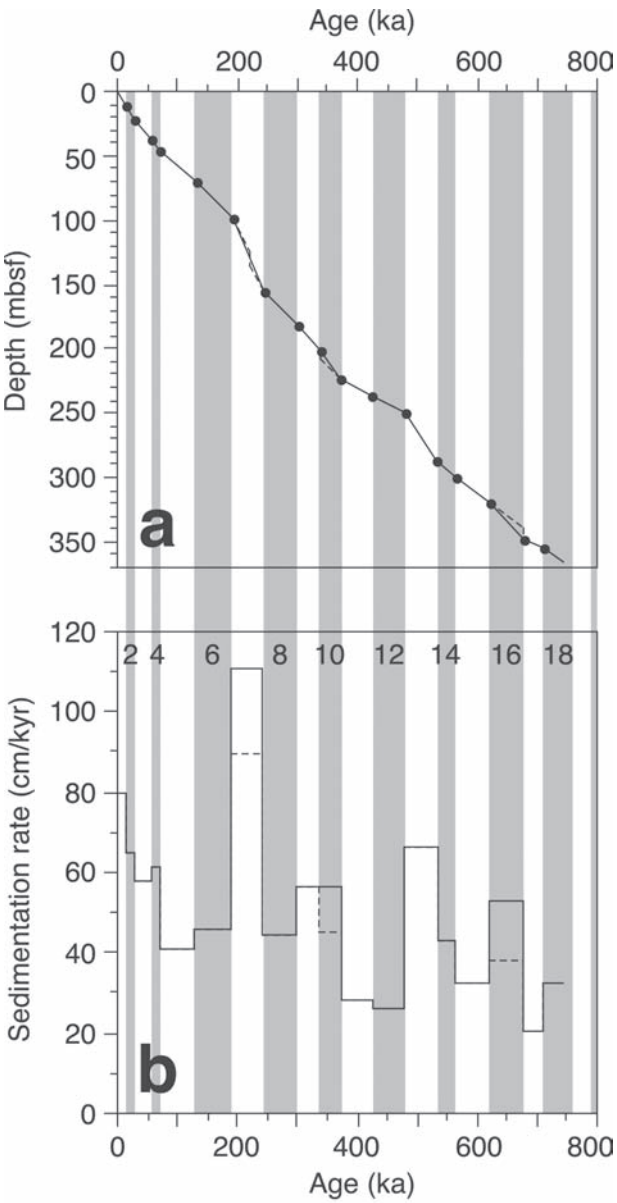

Fig. 3. Depth-age plot (a) and sedimentation rate (b) of C9001C. Glacial stages are shaded. The 18 age-control points are based on correlation of the C9001C benthic $\delta^{18}O$ curve with the LR04 $\delta^{18}O$ curve. Sedimentation rate was calculated based on the depth-age relationship of C9001C: solid line includes slumps and debrites (124–135 mbsf and 203–207 mbsf) and thick sand layers (340–348 mbsf); dotted line excludes these reworked layers.

4. Summary

The stratigraphy of Hole C9001C was established based on a correlation of the C9001C benthic $\delta^{18}O$ curve with the LR04 stack using two tephra layers and two nannofossil datum planes as control points. Hole C9001C provides a nearly continuous record from MIS 18 to the present, with a high mean sedimentation rate of ca. 50 cm/kyr. A middle Pleistocene planktic foraminiferal event, the LO of *N. inglei*, is situated in late MIS 16 or near the MIS 16/15 boundary.

Acknowledgements. Review and comments by three anonymous reviewers significantly helped to improve the manuscript. We express our gratitude to Ms. M. Kobayashi of the Center for Advanced Marine Core Research (CMCR), Kochi University, for technical support in the isotopic measurements. We thank Dr. K. Aoike of the Center for Deep Earth Exploration, Japan Agency for Marine-Earth Science and Technology, Prof. T. Sakai of Utsunomiya University, Prof. H. Yasuda of CMCR, Kochi University, and Ms. Y. Kawate, Mr. K. M. R. Matsuzaki, Dr. N. Suzuki, and Dr. S. Chiyonobu of Tohoku University for assistance with sample preparation. We also thank Dr. R. Asami of Ryukyu University of the Ryukyus for helpful advice concerning stable isotope data. Stable isotope analysis was performed under the cooperative research program of CMCR, Kochi University (Accept Nos. 07B026, 08A027). This research was partly supported by a Grant-in-Aid for Scientific Research (A) from the JSPS, No. 17204043 to M. Oda, and a Grant-in-Aid for Young Scientists (B) from MEXT, No. 20740291 to H. Domitsu, and by the 21st Century Center of Excellence Program "Advanced Science and Technology Center for the Dynamic Earth" of Tohoku University and "Neo-Science of Natural History – Origin and Evolution of Natural Diversity" of Hokkaido University.

References

Aoike, K., 2008. Core samples of D/V CHIKYU Shakedown Cruises offshore Shimokita Peninsula, NE Japan. Gekkan-Chikyu (Earth Monthly) 30, 142–149 (in Japanese).

Aoike, K., Nishi, H., Sakamoto, T., Iijima, K., Tsuchiya, M., Taira, A., Kuramoto, S., Masago, H., Shimokita Core Research Group, 2010. Paleoceanographic history of offshore Shimokita Peninsula for the past 800,000 years based on primary analyses on cores recovered by D/V CHIKYU during the shakedown cruises. Kaseki (Fossils, The Palaeontological Society of Japan) 87, 65–81 (in Japanese with English abstract).

Aoki, K., 2007. Revised age and distribution of ca. 87 ka Aso-4 tephra based on new evidence from the northwest Pacific Ocean. Quaternary International 178, 100–118.

Aoki, K., Arai, F., 2000. Late Quaternary tephrostratigraphy of marine core KH 94-3, LM-8 off Sanriku, Japan. Daiyonki-Kenkyu (The Quaternary Research) 39, 107–120 (in Japanese with English abstract).

Domitsu, H., Oda, M., 2008. Pleistocene planktic foraminiferal events in the northwest Pacific near Japan. The Open Paleontology Journal 1, 1–6.

Fornaciari, E., 2000. Calcareous nannofossil biostratigraphy of the California margin. In: Lyle, M., Koizumi, I., Richter, C., Moore, T.C., Jr. (Eds.), Proceedings of Ocean Drilling Program, Scientific Results, 167. College Station, TX (Ocean Drilling Program), doi:10.2973/odp.proc.sr.167.204.2000.

Kobayashi, S., Ishii, Y., Higuchi, K., Kaminishi, T., Ibusuki, A., Aoike, K., 2009. 2006 Drilling Completion Report Shimokita-West. CDEX Technical Report Vol. 6, Center for Deep Earth Exploration, Japan Agency for Marine-Earth Science and Technology, Yokohama, Japan, 130 pp.

Kucera, M., Kennett, J.P., 2000. Biochronology and evolutionary implications of Late Neogene California margin planktonic foraminiferal events. Marine Micropaleontology 40, 67–81.

Lisiecki, L.E., Raymo, M.E., 2005. A Pliocene – Pleistocene stack of 57 globally distributed benthic $\delta^{18}O$ records. Paleoceanography 20, PA1003, doi:10.1029/2004PA001071.

Lourens, L., Hilgen, F., Shackleton, N.J., Laskar, J., Wilson, D., 2004. The Neogene Period. In: Gradstein, F., Ogg, J., Smith, A. (Eds.), A Geologic Time Scale 2004. Cambridge University Press, Cambridge, UK, pp. 409–440.

Machida, H., 1999. The stratigraphy, chronology and distribution of distal marker-tephras in and around Japan. Global and Planetary Change 21, 71–94.

Oba, T., 1991. The eruption age of the Aso-4 and Ata ashes inferred from oxygen isotope stratigraphy. Gekkan-Chikyu (Earth Monthly) 13, 224–227 (in Japanese).

Raffi, I., Backman, J., Fornaciari, E., Pälike, H., Rio, D., Lourens, L., Hilgen, F., 2006. A review of calcareous nannofossil astrobiochronology encompassing the past 25 million years. Quaternary Science Review 25, 3113–3137.

Sato, T., Kameo, K., Mita, I., 1999. Validity of the latest Cenozoic calcareous nannofossil datums and its application to the tephrochronology. Chikyu-Kagaku (Earth Science) 53, 265–274 (in Japanese with English abstract).

Sato, T., Chiyonobu, S., Hodell, D.A., 2009. Data report: Quaternary calcareous nannofossil datums and biochronology in the North Atlantic Ocean, IODP Site U1308. In: Channell, J.E.T., Kanamatsu, T., Sato, T., Stein, R., Alvarez Zarikian, C.A., Malone, M.J., the Expedition 303/306 Scientists (Eds.), Proceedings of the Integrated Ocean Drilling Program, 303/306. College Station, TX (Integrated Ocean Drilling Program Management International, Inc.), doi:10.2204/iodp.proc.303306.210.2009.

Shackleton, N.J., Opdyke, N.D., 1973. Oxygen isotope and paleomagnetic stratigraphy of Equatorial Pacific core V28-238: oxygen isotope temperatures and ice volumes on a 10^5 and 10^6 year scale. Quaternary Research 3, 39–55.

Wei, W., 1993. Calibration of upper Pliocene – lower Pleistocene nannofossil events with oxygen isotope stratigraphy. Paleoceanography 8, 85–99.

Appendix 1. Oxygen isotopic values for *Uvigerina akitaensis* from the C9001C core. *Uvigerina peregrina* was analyzed only at 202.35 mbsf.

Core-section, interval (cm)	Depth (mbsf)	$\delta^{18}O$ (‰, VPDB)	Core-section, interval (cm)	Depth (mbsf)	$\delta^{18}O$ (‰, VPDB)
1H-1, 24–30	0.27	3.24	8H-4, 90–96	68.70	3.33
1H-2, 50–56	1.92	3.32	8H-5, 45.5–54.5	69.61	3.63
1H-3, 47–53	3.29	3.22	8H-5, 72–78	69.83	3.66
1H-4, 13–19	4.36	3.05	8H-5, 87–93	69.97	3.66
1H-5, 30–36	5.92	3.38	8H-6, 7–13	70.53	4.21
2H-1, 55–61	7.45	3.53	8H-6, 42–48	70.85	4.28
2H-2, 50–56	8.73	3.58	8H-6, 72.5–81.5	71.14	4.54
2H-3, 48–54	10.03	3.98	8H-7, 60.5–69.5	72.36	4.60
2H-4, 31–37	11.21	3.92	9H-1, 60.5–69.5	74.00	4.63
2H-5, 71–77	12.96	4.46	9H-2, 45.5–54.5	75.16	4.56
2H-6, 65–71	14.36	4.60	9H-3, 45.5–54.5	76.45	4.54
2H-7, 47–53	15.61	4.63	9H-4, 45.5–54.5	77.73	4.39
3H-1, 24–30	16.66	4.55	9H-5, 52.5–61.5	79.12	4.54
3H-2, 20–26	17.96	4.50	9H-7, 55.5–64.5	81.74	4.48
3H-3, 47–53	19.58	4.58	10H-1, 45.5–54.5	83.35	4.45
3H-4, 42–48	20.91	4.16	10H-3, 45.5–54.5	85.89	4.30
3H-5, 54–60	22.40	4.34	10H-4, 50.5–59.5	87.22	4.24
3H-6, 50–56	23.74	4.24	10H-5, 45.5–54.5	88.50	4.22
3H-7, 8–14	24.66	4.22	10H-6, 45.5–54.5	89.74	4.16
4H-3, 58–64	29.04	4.05	10H-7, 50.5–59.5	91.04	4.19
4H-4, 62–67	30.36	3.90	11H-1, 41.5–50.5	92.82	4.05
4H-5, 52–58	31.64	4.29	11H-2, 40.5–49.5	94.12	4.29
4H-6, 69–75	33.09	4.21	11H-3, 45.5–54.5	95.52	4.21
4H-7, 47–53	34.18	4.20	11H-5, 45.5–54.5	98.15	3.92
5H-1, 45.5–54.5	35.86	4.28	12H-1, 45.5–54.5	102.36	3.86
5H-2, 40.5–49.5	37.10	4.24	12H-2, 45.5–54.5	103.62	3.77
5H-3, 45.5–54.5	38.44	4.33	12H-3, 60.5–69.5	105.02	3.59
5H-4, 45.5–54.5	39.76	4.38	12H-4, 20.5–29.5	105.96	3.67
5H-5, 63.5–72.5	41.28	4.30	12H-5, 45.5–54.5	107.53	3.67
5H-6, 55.5–64.5	42.58	4.31	12H-6, 20.5–29.5	108.77	3.78
5H-7, 45.5–54.5	43.76	4.31	12H-7, 55.5–64.5	110.35	3.94
6H-1, 80.5–89.5	45.69	4.05	13H-1, 57.5–66.5	111.97	3.85
6H-2, 61.5–70.5	46.79	4.10	13H-2, 45.5–54.5	113.22	3.82
6H-3, 7.5–16.5	47.57	4.07	13H-3, 45.5–54.5	114.51	3.76
6H-4, 45.5–54.5	49.25	4.00	13H-4, 45.5–54.5	115.80	3.58
6H-5, 45.5–54.5	50.60	3.76	13H-5, 45.5–54.5	117.12	3.58
6H-6, 45.5–54.5	51.93	3.79	13H-6, 40.5–49.5	118.37	3.47
6H-7, 40.5–49.5	53.19	3.76	13H-7, 35.5–44.5	119.62	3.65
7H-1, 47.5–56.5	54.88	4.09	14H-3, 47–53	123.93	3.99
7H-2, 53.5–62.5	56.20	4.04	14H-4, 47–53	125.26	4.16
7H-3, 65.5–74.5	57.67	3.87	14H-5, 47–53	126.63	4.06
7H-4, 45.5–54.5	58.77	3.84	14H-6, 67–73	128.18	3.67
7H-5, 45.5–54.5	60.22	3.77	14H-7, 47–53	129.27	3.61
7H-6, 50.5–59.5	61.54	3.84	15H-2, 22–28	130.83	4.17
7H-7, 45.5–54.5	62.77	3.97	15H-3, 65.5–74.5	131.54	4.04
8H-1, 45.5–54.5	64.37	3.40	15H-4, 65.5–74.5	132.74	4.04
8H-2, 70.5–79.5	65.94	3.22	15H-5, 37–43	133.65	3.97
8H-3, 45.5–54.5	67.02	3.02	15H-7, 47–53	136.25	4.49
8H-3, 73–79	67.26	3.16	15H-8, 37–43	137.47	4.55
8H-3, 96–102	67.47	3.12	15H-9, 45.5–54.5	138.80	4.34
8H-4, 26–32	68.12	3.22	16H-2, 10–16	140.33	3.82
8H-4, 45.5–54.5	68.31	3.57	16H-3, 37–43	141.80	4.12

Core-section, interval (cm)	Depth (mbsf)	$\delta^{18}O$ (‰, VPDB)
16H-4, 47–53	143.14	4.07
16H-5, 57–63	144.58	3.87
16H-6, 37–43	145.74	4.04
16H-8, 62–68	148.57	4.51
17H-2, 24–30	149.80	4.27
17H-3, 37–43	151.20	4.06
17H-4, 37–43	152.47	3.82
17H-5, 37–43	153.75	3.95
17H-6, 42–48	155.08	3.35
17H-7, 42–48	156.38	4.37
17H-8, 49–55	157.72	4.26
18H-1, 47–53	159.35	4.28
18H-2, 42–48	160.56	4.20
18H-3, 42–48	161.78	4.18
18H-4, 42–48	163.04	4.31
18H-5, 37–43	164.31	4.12
19H-1, 57–63	165.97	4.04
19H-2, 35–41	167.04	3.95
19H-3, 50–56	168.51	4.10
19H-4, 70–76	170.02	3.95
19H-5, 38–44	171.04	3.79
19H-6, 47–53	172.44	3.77
19H-7, 42–48	173.74	3.92
20H-2, 7–13	175.53	4.01
20H-3, 62–68	176.89	4.00
20H-4, 47–53	178.15	3.96
20H-5, 43–49	179.52	4.08
20H-6, 42–48	180.93	3.96
20H-7, 37–43	182.30	3.76
20H-8, 32–38	183.66	4.10
21H-1, 47–53	184.86	3.76
21H-2, 58–64	186.32	3.66
21H-3, 67–73	187.77	3.53
21H-4, 47–53	188.96	3.42
21H-5, 56–62	190.51	3.38
21H-6, 47–53	191.70	3.27
21H-7, 45–51	192.96	3.21
22H-1, 27–33	194.18	3.11
22H-2, 89–95	195.10	3.15
22H-3, 47–53	195.99	3.18
22H-4, 47–53	197.26	3.18
22H-5, 48–54	198.53	3.27
22H-6, 52–58	199.85	3.24
22H-7, 47–53	201.08	3.27
22H-8, 47–53	202.35	4.68
23H-1, 47–53	203.86	4.22
23H-2, 72–78	205.34	3.95
23H-3, 37–43	206.29	3.52
23H-4, 57–63	207.73	3.60
23H-5, 54–60	208.97	4.66
23H-6, 37–43	210.08	4.48
23H-7, 52–58	211.47	4.36
24H-1, 25–31	213.16	4.28
24H-2, 53–59	214.73	4.16
24H-3, 7–13	215.59	4.26
24H-3, 115–121	216.57	4.07
24H-5, 21–27	218.24	4.12
24H-6, 62–68	219.89	4.20
24H-7, 41–47	220.96	4.10
25H-1, 5–11	222.48	4.06
25H-1, 20–26	222.61	4.02
25H-2, 8–14	222.95	3.84
25H-2, 37–43	223.20	4.15
25H-3, 47–53	224.51	3.94
25H-4, 9–15	225.40	3.92
25H-4, 84–90	226.05	3.86
25H-5, 5–11	226.59	3.74
25H-5, 89–95	227.32	3.81
25H-6, 10–16	227.87	3.86
25H-6, 47–53	228.19	3.56
25H-6, 97–103	228.62	4.18
25H-7, 10–16	229.09	3.97
25H-7, 62–68	229.55	3.23
25H-7, 114–120	230.00	3.34
25H-8, 49–55	230.69	3.34
25H-8, 108–114	231.21	3.31
26H-1, 23–29	232.14	3.46
26H-1, 52–58	232.39	3.51
26H-2, 47–53	233.59	3.56
26H-2, 98–104	234.04	3.60
26H-3, 17–23	234.49	3.82
26H-3, 57–63	234.85	3.78
26H-3, 107–113	235.29	3.81
26H-4, 13–19	235.71	3.94
26H-4, 47–53	236.01	3.92
26H-4, 107–113	236.53	3.97
26H-5, 10–16	236.93	4.40
26H-5, 51–57	237.29	4.55
26H-5, 90–96	237.63	4.52
26H-6, 4–10	238.12	4.62
26H-6, 27–33	238.32	4.76
26H-6, 48–54	238.50	4.67
27H-1, 10–16	239.15	4.62
27H-1, 47–53	239.49	4.43
27H-1, 127–133	240.22	4.40
27H-2, 32–38	240.71	4.31
27H-3, 47–53	242.14	4.36
27H-4, 67–73	243.62	4.26
27H-4, 107–113	243.98	4.25
27H-5, 47–53	244.72	4.09
27H-6, 47–53	246.07	4.18
27H-6, 69–75	246.27	4.28
27H-7, 38–44	247.10	4.04
27H-8, 24–30	248.17	4.13
28H-1, 57–63	249.07	4.14
28H-2, 47–53	250.27	4.03
28H-2, 87–93	250.63	3.92
28H-3, 87–93	251.90	3.80

Core-section, interval (cm)	Depth (mbsf)	$\delta^{18}O$ (‰, VPDB)
28H-4, 67–73	252.99	3.92
28H-5, 47–53	254.13	3.75
28H-6, 47–53	255.51	3.86
28H-7, 67–73	256.96	3.75
28H-7, 107–113	257.32	3.66
29H-1, 1–7	258.07	3.47
29H-2, 47–53	259.30	3.63
29H-3, 37–43	260.61	3.55
29H-4, 47–53	262.12	3.57
29H-5, 37–43	263.42	3.74
29H-6, 82–88	265.27	3.68
30H-1, 24–30	267.76	4.01
30H-2, 77–83	269.39	3.86
30H-3, 67–73	270.49	3.78
30H-4, 37–43	271.41	3.76
30H-5, 47–53	272.68	3.92
30H-6, 37–43	273.78	4.00
31H-1, 37–43	274.68	3.85
31H-2, 25–31	275.79	3.92
31H-3, 77–83	277.45	3.56
31H-4, 47–53	278.35	3.51
31H-5, 42–48	279.47	3.58
31H-6, 47–53	280.69	3.52
31H-7, 47–53	281.82	3.58
32H-1, 22–28	282.88	3.71
32H-2, 99–105	284.63	3.72
32H-3, 68–74	285.64	3.75
32H-4, 77–83	287.03	3.80
32H-6, 32–38	289.20	4.13
32H-7, 37–42	290.46	3.95
32H-8, 36–42	291.60	3.89
33H-1, 37–43	292.52	3.95
33H-2, 67–73	293.82	4.00
33H-3, 47–53	295.05	4.42
33H-4, 67–73	296.52	4.27
33H-5, 78–84	297.86	4.18
33H-6, 57–63	298.98	4.15
33H-7, 14–20	299.87	3.86
33H-8, 26–32	300.70	3.97
34X-2, 8–14	302.05	3.74
34X-3, 22–28	303.20	3.66
34X-4, 35–41	304.76	3.66
34X-5, 37–43	306.19	3.71
34X-6, 42–48	307.64	3.65
34X-8, 17–23	309.60	3.56
35X-1, 18–24	311.37	3.68
35X-2, 12–18	311.71	4.11
35X-2, 70–76	312.29	3.78
35X-2, 99–105	312.58	4.03
35X-3, 97–103	313.89	4.00
35X-4, 12–18	314.45	3.92
35X-4, 57–63	314.90	3.71
35X-4, 92–98	315.25	3.81
35X-5, 12–18	315.86	3.99
35X-5, 47–53	316.21	4.07
35X-5, 100–106	316.74	3.69
35X-6, 10–16	317.26	3.54
35X-6, 42–48	317.58	3.93
35X-6, 88–94	318.04	4.05
35X-7, 4–10	318.62	3.97
35X-7, 16–22	318.74	4.21
35X-7, 34–40	318.92	4.11
37X-1, 18–24	330.37	4.69
37X-1, 40–46	330.59	4.61
37X-1, 87–93	331.06	4.63
37X-2, 30–36	331.78	4.60
37X-2, 75–81	332.23	4.59
37X-2, 94–100	332.42	4.76
37X-3, 48–54	333.37	4.29
37X-3, 92–98	333.81	4.57
37X-4, 12–18	334.40	4.53
37X-4, 108–114	335.36	4.53
37X-4, 117–123	335.45	4.53
37X-5, 7–13	335.76	4.49
37X-5, 27–33	335.96	4.30
37X-5, 47–53	336.16	4.80
37X-5, 97–103	336.66	4.66
37X-6, 11–17	337.13	4.52
37X-6, 29–35	337.31	4.40
37X-6, 48–54	337.50	4.43
38H-3, 22–28	342.46	4.30
39H-1, 8–14	347.74	4.15
39H-1, 75–81	348.41	4.10
39H-1, 92–98	348.58	4.08
39H-2, 27–33	349.42	4.02
39H-3, 22–28	349.99	4.05
39H-3, 36–42	350.13	4.05
39H-4, 17–23	350.38	4.10
39H-5, 22–28	351.00	3.68
39H-5, 57–63	351.35	4.15
39H-6, 7–13	351.54	3.92
39H-6, 23–29	351.70	3.92
39H-6, 42–48	351.89	3.85
39H-7, 10–16	352.09	3.84
39H-7, 29–35	352.28	3.88
39H-8, 10–16	352.45	3.48
39H-8, 22–28	352.57	3.15
39H-9, 16–22	352.84	3.66
39H-9, 28–34	352.96	3.72
39H-10, 19–25	353.23	3.59
39H-11, 17–23	353.48	3.66
39H-12, 27–33	353.94	3.76
39H-13, 24–30	354.36	3.59
40H-1, 4–10	355.90	4.45
40H-1, 16–22	356.01	4.34
40H-2, 2–8	356.10	4.45
40H-2, 30–36	356.37	4.46
40H-2, 115–121	357.19	4.42

Core-section, interval (cm)	Depth (mbsf)	$\delta^{18}O$ (‰, VPDB)
40H-3, 52–58	357.94	4.42
40H-3, 85–91	358.26	4.69
40H-3, 98–104	358.39	4.65
40H-4, 57–63	359.35	4.48
40H-4, 92–98	359.69	4.48
40H-4, 117–123	359.93	4.43
40H-5, 5–11	360.21	4.27
40H-5, 12–18	360.28	4.35
40H-6, 5–11	360.45	4.32
40H-8, 15–21	361.47	4.13
40H-8, 28–34	361.60	4.17
40H-9, 30–36	362.34	4.18
40H-10, 30–36	362.94	4.34
40H-10, 55–61	363.18	4.26
40H-12, 5–11	364.07	4.09
40H-12, 18–24	364.19	4.15
40H-12, 35–41	364.36	4.07
40H-13, 3–9	364.48	4.09
40H-13, 24–30	364.68	4.15
40H-14, 18–24	364.93	4.11

Manuscript received: April 4, 2010; rev. version accepted: October 15, 2010.